

Loss of Primary Cilia Drives Switching from Hedgehog to Ras/MAPK Pathway in Resistant Basal Cell Carcinoma

François Kuonen^{1,2}, Noelle E. Huskey^{1,2}, Gautam Shankar¹, Prajakta Jaju¹, Ramon J. Whitson¹, Kerri E. Rieger^{1,3}, Scott X. Atwood^{1,4}, Kavita Y. Sarin¹ and Anthony E. Oro¹

Basal cell carcinomas (BCCs) rely on Hedgehog (HH) pathway growth signal amplification by the microtubule-based organelle, the primary cilium. Despite naive tumor responsiveness to Smoothed inhibitors (Smoⁱ), resistance in advanced tumors remains common. Although the resistant BCCs usually maintain HH pathway activation, squamous cell carcinomas with Ras/MAPK pathway activation also arise, and the molecular basis of tumor type and pathway selection are still obscure. Here, we identify the primary cilium as a critical determinant controlling tumor pathway switching. Strikingly, Smoothed inhibitor-resistant BCCs have an increased mutational load in ciliome genes, resulting in reduced primary cilia and HH pathway activation compared with naive or Gorlin syndrome patient BCCs. Gene set enrichment analysis of resistant BCCs with a low HH pathway signature showed increased Ras/MAPK pathway activation. Tissue analysis confirmed an inverse relationship between primary cilia presence and Ras/MAPK activation, and primary cilia removal in BCCs potentiated Ras/MAPK pathway activation. Moreover, activating Ras in HH-responsive cell lines conferred resistance to both canonical (vismodegib) and noncanonical (atypical protein kinase C and MRTF inhibitors) HH pathway inhibitors and conferred sensitivity to MAPK inhibitors. Our results provide insights into BCC treatment and identify the primary cilium as an important lineage gatekeeper, preventing HH-to-Ras/MAPK pathway switching.

Journal of Investigative Dermatology (2019) ■, ■–■; doi:10.1016/j.jid.2018.11.035

INTRODUCTION

Basal cell carcinoma (BCC) is the most common skin cancer, affecting more than 50% of Caucasians during their lifetime (Kasper et al., 2012). BCCs depend on a deregulated Hedgehog (HH) signaling pathway, leading to Smoothed (Smo) de-repression and the activation of Gli transcription factors (Epstein, 2008; Rubin and de Sauvage, 2006). Facilitating high pathway output is the primary cilium, a microtubule-based organelle in which the core components of the HH pathway co-localize upon signal transduction (Bangs and Anderson, 2017; Pak and Segal, 2016; Wu et al., 2017). Intense study over the past decade shows the necessity of the primary cilium for HH pathway activity, because human ciliopathies phenocopy HH mutations.

Although Smo inhibitors (Smoⁱ) potently prevent naive BCC growth (Migden et al., 2015; Rubin and de Sauvage, 2006), resistance emerges rapidly, with early and advanced sporadic BCCs showing 40% and 60% resistance, respectively (Axelson et al., 2013; Chang and Oro, 2012; Sekulic et al., 2012; Tang et al., 2012). Although sensitive BCCs harbor reduced HH pathway activation under Smoⁱ (Migden et al., 2015), detailed genomic interrogation of Smoⁱ-resistant BCCs has identified both genetic alterations in Smo and downstream compensatory mechanisms that maintain BCC growth through HH pathway activation. These include point mutations in Smoⁱ binding-pocket or Smo-activating mutations (Atwood et al., 2015; Sharpe et al., 2015; Yauch et al., 2009), amplification of Gli2 or the HH target gene cyclin D1 (Buonamici et al., 2010; Dijkgraaf et al., 2011), and non-canonical mechanisms to bolster HH pathway output through enhanced phosphoinositide 3 kinase, atypical protein kinase C signaling, or G actin-mediated activation of the MRTF/SRF complex (Atwood et al., 2013; Buonamici et al., 2010; Whitson et al., 2018). These results show the diverse mechanisms used to maintain Gli activity in resistant BCCs and suggest the existence of other as yet undiscovered resistance pathways.

An emerging route to Smoⁱ resistance occurs through the switching of BCC to squamous cell carcinoma (SCC) (Otsuka et al., 2015; Ransohoff et al., 2015; Saintes et al., 2015; Zhao et al., 2015). Primarily seen in patients with sporadic, not syndromic, BCCs, SCC that arise during Smoⁱ treatment has been found by multiple independent studies to share high sequence similarity to the naive BCC, supporting the idea that these SCCs emerge directly from the naive BCC (Ransohoff

¹Program in Epithelial Biology and Department of Dermatology, Stanford University School of Medicine, Stanford, California, USA; and ²Department of Pathology, Stanford University School of Medicine, Stanford, California, USA

³These authors contributed equally to this work.

⁴Current address: Department of Developmental and Cell Biology, University of California, Irvine, Irvine, California, USA.

Correspondence: Anthony E. Oro, Program in Epithelial Biology and Department of Dermatology, Stanford University School of Medicine, Stanford, California, USA. E-mail: oro@stanford.edu

Abbreviations: 4OHT, 4-hydroxy-tamoxifen; BCC, basal cell carcinoma; CBD, ciliobrevin D; Dox, doxycycline; GSEA, Gene Set Enrichment Analysis; HH, Hedgehog; MEK, MAPK/ERK kinase; SCC, squamous cell carcinoma; Smo, Smoothed; Smoⁱ, Smoothed inhibitor

Received 28 August 2018; revised 8 November 2018; accepted 9 November 2018; accepted manuscript published online 29 January 2019; corrected proof published online XXX

et al., 2015; Zhao et al., 2015). Rather than HH dependence for cell growth, SCCs depend instead on the Ras/MAPK pathway activation and loss of Notch signaling for proliferation and blocking of differentiation, respectively (Lee et al., 2014; Lefort et al., 2007). Although previous work in transgenic mice illustrates how Ras pathway blockade in the context of SCC development leads to hair follicle-lineage sebaceous adenomas with increased HH signaling (Gerdes et al., 2006), the factors determining BCC-to-SCC pathway switching in the human tumor setting remain mysterious.

In this study, we found increased levels of mutations in genes encoding the ciliome and reduced primary cilia in human resistant BCC. Loss of cilia was correlated with lower HH and higher Ras/MAPK pathway activation. Consistently, both pharmacological and genetic depletions of primary cilia inhibit the HH pathway and potentiate Ras/MAPK pathway activation. Using GLI-dependent cell lines, we show that Ras/MAPK pathway activation confers resistance to both canonical and noncanonical HH pathway inhibitors and confers sensitivity to MAPK/ERK kinase (MEK) inhibitors, suggesting a switch from a GLI-dependent to a GLI-independent cell state. Altogether, these results identify primary cilia as gatekeepers between the HH and Ras/MAPK signaling pathways in BCC. They support the switch to the Ras/MAPK pathway as a potential mechanism of resistance to both canonical and non-canonical HH pathway inhibitors.

RESULTS

Human resistant BCCs harbor reduced primary cilia

We have previously observed that the rate of resistance to Smoⁱ differed dramatically between different patient populations, with syndromic Gorlin syndrome patients showing significantly less resistance despite hundreds of tumors (Tang et al., 2012). To gain insight into the basis of this resistance, we submitted our previously identified list of genes commonly mutated in resistant BCCs (Atwood et al., 2015) (Gene Expression Omnibus [GEO] accession number GSE58377) (see Supplementary Table S1 online) to gene ontology analysis. Analyses for both cellular component and molecular function highlighted constitutive and functional components of the primary cilium (Figure 1a). To quantify mutations in ciliary genes, we reported the mutations in the coding sequences of the 303 ciliary genes comprised by the SYSCILIA list (van Dam et al., 2013) for Gorlin syndrome patients and sporadic naive and vismodegib-resistant BCCs (National Institutes of Health Sequence Read Archive SAMN07507265–AMN07507288, GEO accession number GSE58377) (see Supplementary Figure S1a online). The mutation rates found in the ciliome (5.73 and 13.29 mutations/megabases (Mb) for Gorlin syndrome patients and sporadic BCCs, respectively) were significantly lower than the genome-wide mutation rates previously reported in BCCs (21 and 65 mutations/Mb, respectively) (Bonilla et al., 2016), indicating that the ciliome is conserved during the early stages of BCC progression. This is consistent with the prominent role of cilia for HH pathway activation and maintenance. However, ciliome mutations were found in significantly higher numbers in resistant compared with sporadic or Gorlin syndrome patient BCCs (Figure 1b),

including when controlling for the large gene size of ciliary protein-encoding genes.

To confirm that these sequence alterations in ciliome components were reflected in altered ciliogenesis, we compared Gorlin syndrome patients and sporadic naive and resistant BCCs for cilia by immunostaining. Consistent with the sequencing data, we found that resistant BCCs harbored significantly reduced cilia number (Figure 1c). To question the potential contribution of Smoⁱ in reduced ciliogenesis (Otsuka et al., 2015), we compared primary cilia in both the tumor and stromal compartments. Cilia were lost specifically in the tumor epithelium and not in the stromal compartment (Figure 1d, and see Supplementary Figure S1b). Moreover, Gorlin syndrome patient BCCs treated with Smoⁱ harbored conserved cilia relative to resistant BCC, despite efficient HH pathway inhibition, evaluated by nuclear Gli1 staining intensity (see Supplementary Figure S1c and d). Finally, because ciliogenesis may be affected by a higher proliferation rate, we compared the proliferation rates of sporadic naive versus resistant BCCs using Ki67 immunostaining and failed to detect differences (see Supplementary Figure S1e). Altogether, these observations suggest a major contribution of the genetic mutations rather than the Smoⁱ therapy or the proliferation status in the reduced ciliogenesis observed in resistant BCCs.

Loss of primary cilia correlates with HH pathway inactivation and Ras/MAPK pathway activation in a subset of resistant BCCs

The observation of reduced cilia questions previous demonstration that BCCs uniformly depend on the HH pathway for growth; indeed, all Smoⁱ resistant BCCs our group and others have characterized maintain or up-regulate HH pathway target genes (Atwood et al., 2015; Sharpe et al., 2015). This led us to investigate alternative signaling mechanisms on which BCCs with altered cilia depend for growth, a phenomenon well characterized in many tumor types as pathway switching (Chandarlapaty, 2012; Chandarlapaty et al., 2011; Serra et al., 2011). Our group and others previously reported the emergence of SCCs from vismodegib-treated BCCs (Otsuka et al., 2015; Ransohoff et al., 2015; Zhao et al., 2015). Because the Ras/MAPK pathway is a main driver of SCC progression (Lee et al., 2014; Lefort et al., 2007; Pickering et al., 2014) and was shown to promote resistance to sonidegib, a Smoⁱ, in an experimental model of medulloblastoma (Zhao et al., 2015), we hypothesized that BCC may transition from the HH to Ras/MAPK pathway upon Smoⁱ therapy.

To determine whether the Ras pathway was activated in resistant BCC, we used previously obtained RNA sequencing data (GEO accession number GSE58377) (Atwood et al., 2015). Because the Ras pathway is activated during normal skin differentiation, we decided to compare transcriptomes of resistant to sporadic naive BCC samples (rather than normal skin) obtained from the same patient. In this setting, we identified seven matched pairs. When the RNA sequencing data were analyzed together, Gene Set Enrichment Analysis (GSEA) identified the HH pathway (as previously reported in Atwood et al. [2015] and Sharpe et al. [2015]) but failed to identify Ras pathway activation in resistant BCCs (see

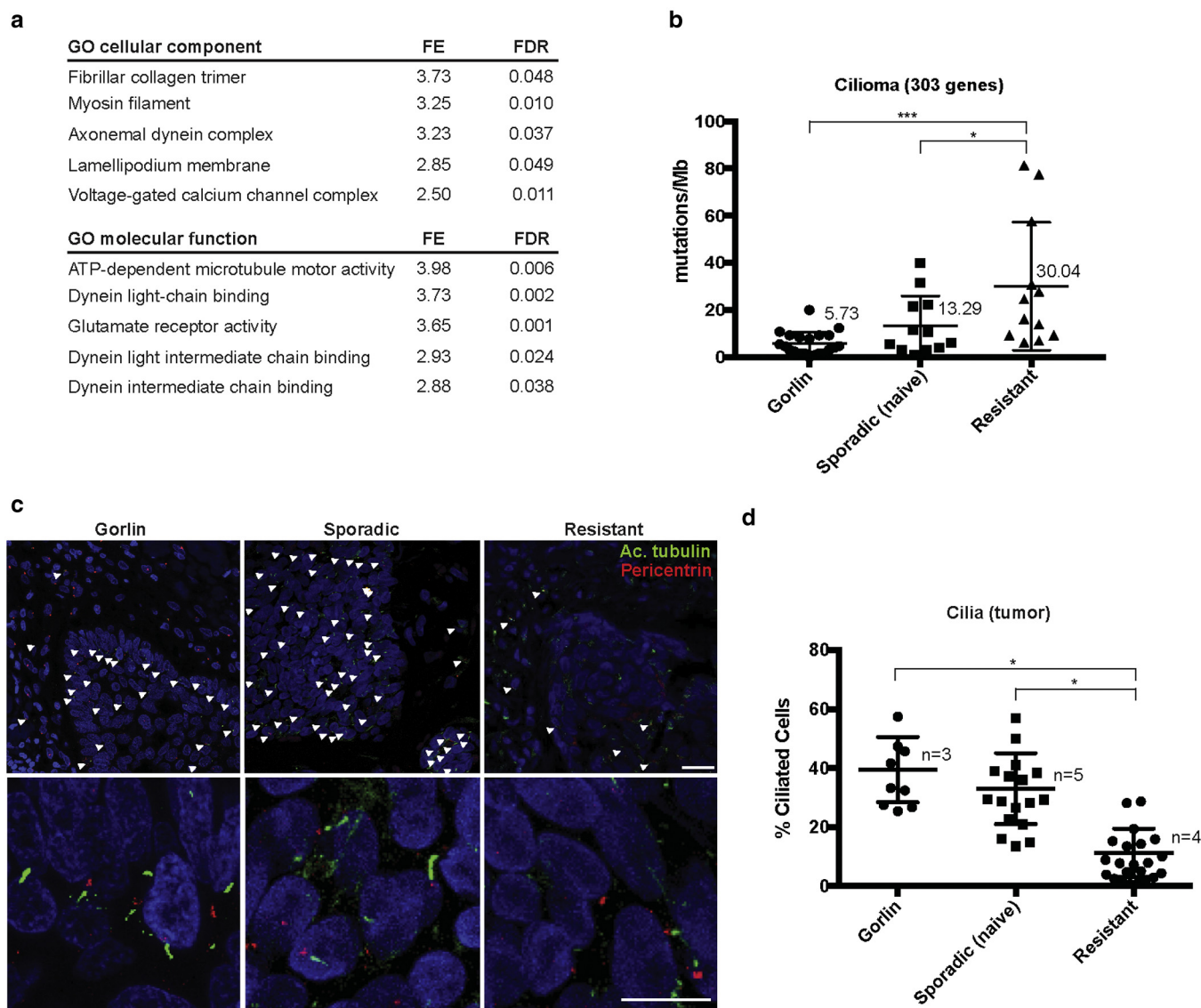


Figure 1. Human resistant BCC harbor reduced primary cilia. (a) Top lists of GO cellular components and molecular functions associated with genes commonly mutated in resistant BCCs. (b) Quantification of the mutations found in the ciliome of Gorlin syndrome patient and sporadic naive and resistant human BCCs with whole-exome sequencing. Numbers indicate the mean values for each category. (c) Acetylated tubulin (cilia shaft), pericentrin (cilia body), and DAPI immunostainings of Gorlin syndrome patient, sporadic naive, and resistant human BCCs. White arrowheads indicate cilia. (d) Quantification of cilia in the tumor compartment shown in c. Dots represent microscope fields, distributed across $n \geq 3$ tumors. Scale bars indicate 25 μm . Horizontal bars and error bars in **b** and **d** represent the mean \pm standard deviation. * $P < 0.05$, *** $P < 0.001$. Ac., acetylated; ATP, adenosine triphosphate; BCC, basal cell carcinoma; FDR, false discovery rate; FE, fold enrichment; GO, gene ontology; Mb, megabase.

Supplementary Figure S2a online). However, we may reasonably expect the activation of the Ras pathway to occur as an alternative rather than an additional mechanism to HH pathway activation in resistant BCC. Therefore, we distinguished HH-high paired samples, defined by a significant enrichment for the HH pathway (normalized enrichment score [NES] > 1 and $P < 0.05$) from HH-low paired samples (NES < 1 or $P > 0.05$) (Figure 2a). When analyzed separately, we confirmed the absence of Ras pathway enrichment in the HH-high group, whereas the Ras pathway was significantly enriched in the HH-low group (Figure 2b, and see Supplementary Figure S2b online).

To further document their reciprocal relationship, we quantified cilia, nuclear Gli1 (as readout for HH pathway activation) (see Supplementary Figure S1d) and

phosphorylated (p-) MEK (as readout for Ras/MAPK pathway activation) (see Supplementary Figure S1d) in various areas across resistant BCCs on immediate adjacent sections. Overall, cilia, nuclear Gli1, and p-MEK immunostainings showed intra- and intertumoral heterogeneity. Nuclear Gli1 and p-MEK immunostainings showed a noncontinuous inverse correlation identifying both Gli1^{high}/p-MEK^{low} and Gli1^{low}/p-MEK^{high} areas ($n = 43$ sections examined) (Figure 2c and d, and see Supplementary Figure S2c). Cilia were mostly conserved in the Gli1^{high}/p-MEK^{low} areas and mostly lost in the Gli1^{low}/p-MEK^{high} areas (Figure 2c and d). As expected, primary cilia showed a significant positive correlation with HH pathway activation (Spearman correlation factor = 0.80) (see Supplementary Figure S2d) but a significant negative correlation with Ras/MAPK pathway

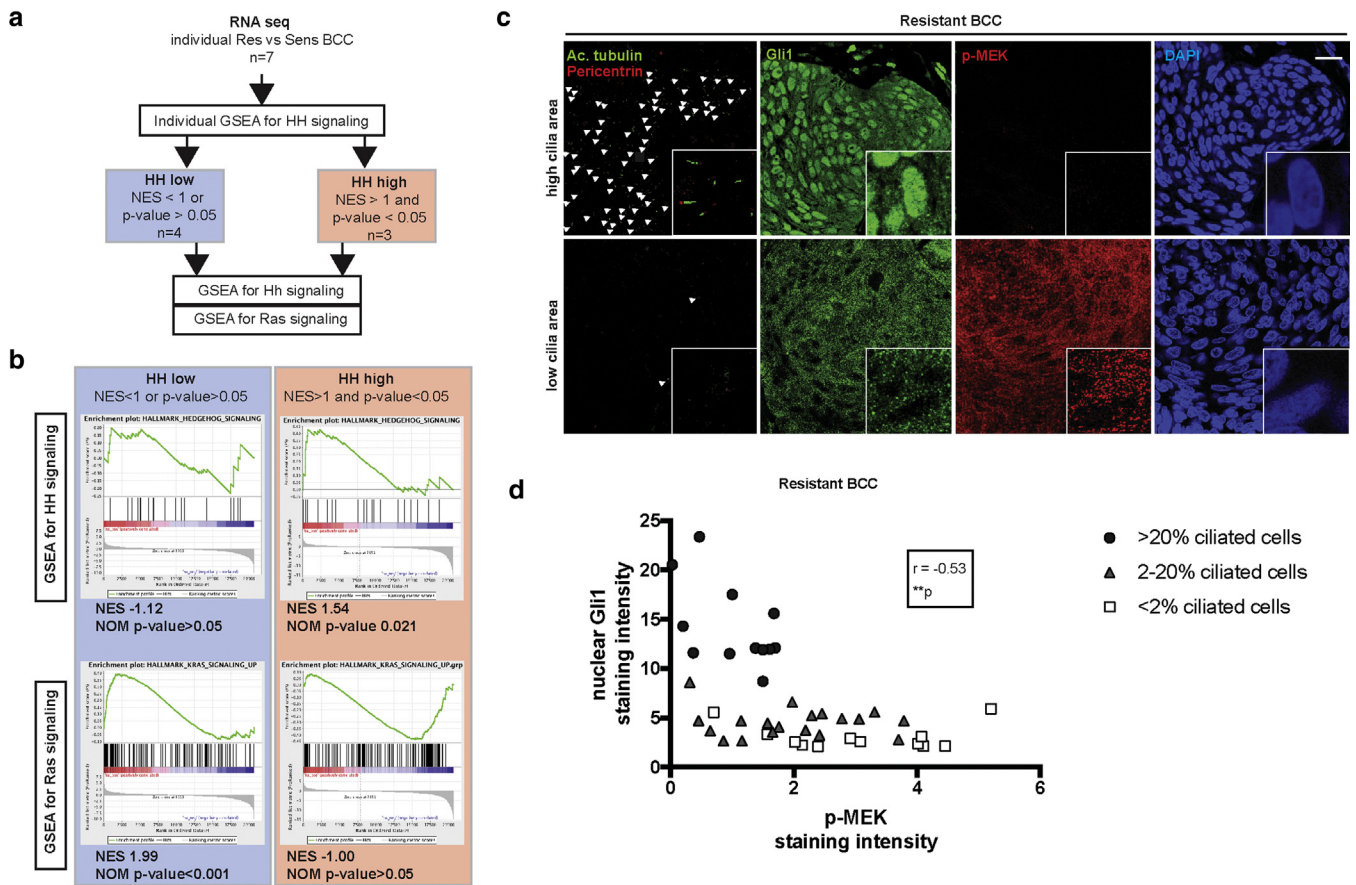


Figure 2. Loss of primary cilia goes with HH pathway inactivation and Ras/MAPK pathway activation in a subset of resistant BCCs. (a) Algorithm for the analysis of RNA sequencing obtained from vismodegib-sensitive and -resistant human BCCs. (b) GSEA for HH and Ras pathways activation in HH-high versus HH-low human resistant BCCs. NES stands for normalized enrichment score. (c) Adjacent immunostainings for cilia (acetylated tubulin and pericentrin), Gli1 (as a readout for HH pathway activation), and p-MEK (as readout for Ras/MAPK pathway activation) in resistant human BCCs. White arrowheads indicate cilia. Higher magnifications are shown in framed pictures. (d) Correlation between nuclear Gli1 and p-MEK relative intensity in resistant human BCCs, annotated for cilia density. Dots represent microscope fields, distributed across four different resistant BCC tumors. Scale bar = 25 μ m. ** $P < 0.01$; r indicates the Spearman correlation factor. Ac., acetylated; BCC, basal cell carcinoma; GSEA, Gene Set Enrichment Analysis; HH, Hedgehog; MEK, MAPK/ERK kinase; NES, normalized enrichment score; p-, phosphorylated; Res, vismodegib resistant; RNA-seq, RNA sequencing; Sens, vismodegib sensitive.

activation (Spearman correlation factor = -0.61) (see [Supplementary Figure S2e](#)). Altogether, our results identify an antagonistic relationship between the cilia/HH pathway and Ras/MAPK pathway in a subset of resistant BCCs.

Loss of primary cilia potentiates Ras/MAPK pathway activation in resistant BCC cell lines

Our sequencing and histological results suggest a strong reciprocal relationship between the presence of normal cilia/HH pathway activation and Ras/MAPK pathway activation. To confirm the cilia dependency of the HH pathway in vitro, we used the GLI-dependent murine (ASZ) and human (UWBCC) BCC cell lines. First, we mimicked loss of cilia using ciliobrevin D (CBD), a cytoplasmic dynein inhibitor known to impede cilia formation ([Fu et al., 2014](#)). Both ASZ and UWBCC cell lines showed a dose-dependent reduction in both the fraction of ciliated cells and the cilia length upon CBD treatment (see [Supplementary Figure S3a–c](#) online). To determine the HH pathway response upon CBD treatment, we performed RNA sequencing on ASZ upon DMSO (control) or CBD (10 μ mol/L) (GEO accession number GSE120954). GSEA showed a significant negative

enrichment for the HH pathway upon CBD ([Figure 3a](#)), showing HH pathway inactivation upon loss of cilia. This was confirmed in both the ASZ and UWBCC cell lines, which showed a dose-dependent reduction in Gli1 mRNA in response to CBD treatment (see [Supplementary Figures S3d](#) and e). To confirm these results, we tested a complementary genetic approach, using mRNA silencing of OFD1, a gene essential for primary cilia formation ([Ferrante et al., 2006](#)). OFD1 small interfering RNA efficiently silenced OFD1 mRNA (see [Supplementary Figure S3f](#) and g), prevented cilia formation (see [Supplementary Figure S3h](#) and j) and inhibited HH pathway activation in both ASZ and UWBCC cells (see [Supplementary Figure S3k](#)), confirming the cilia dependency of the HH pathway in GLI-dependent BCC cell lines.

We then wondered whether loss of cilia may affect Ras/MAPK pathway activation as well. Therefore, we first used the RNA-sequencing data obtained from ASZ cells lines upon DMSO (control) or CBD (10 μ mol/L) (GEO accession number GSE120954). GSEA for Ras pathway activation did not show any significant enrichment upon CBD treatment ([Figure 3b](#)), indicating that loss of cilia fails to elicit Ras pathway

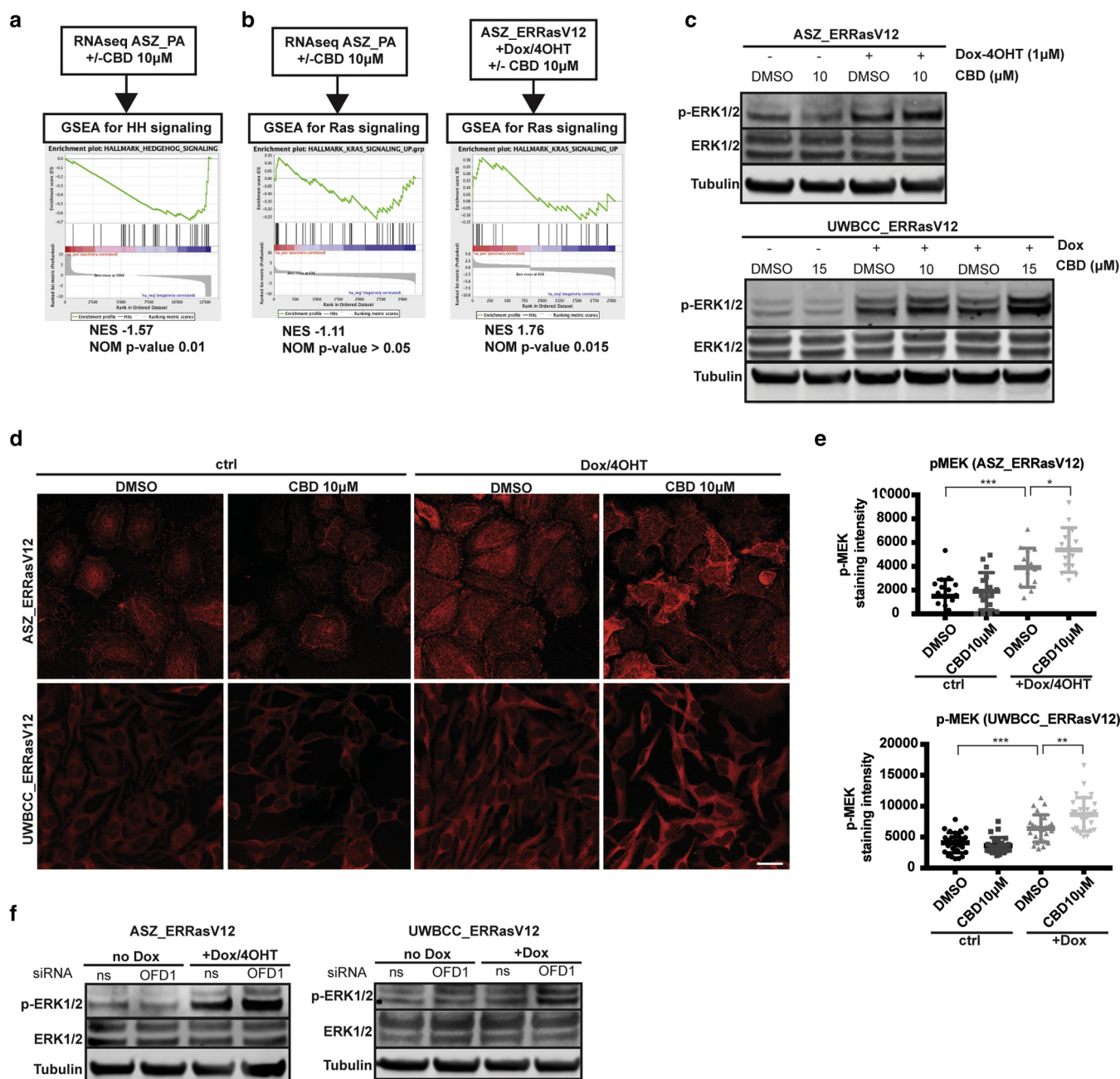


Figure 3. Loss of primary cilia potentiates Ras/MAPK pathway activation. (a) GSEA for HH pathway activation in RNA-sequencing data obtained from ASZ_PA upon DMSO (control) versus CBD (10 µmol/L) treatment. (b) GSEA for Ras pathway activation in RNA-sequencing data obtained from ASZ_PA or ASZ_ERRasV12/Dox-4OHT upon DMSO (control) versus CBD (10 µmol/L) treatment. (c) Western blot for p-ERK1/2 (as readout for Ras/MAPK pathway activation), total ERK1/2 and β tubulin (loading control) in ASZ_ERRasV12 and UWBC_ERRasV12 upon doxycycline/4OHT and DMSO (control) versus CBD treatment. (d) p-MEK immunostaining (as readout for Ras/MAPK pathway activation) in ASZ_ERRasV12 and UWBC_ERRasV12 upon doxycycline/4OHT and DMSO (control) versus CBD treatment. (e) Quantification of p-MEK immunostaining in ASZ_ERRasV12 and UWBC_ERRasV12 upon doxycycline/4OHT and DMSO (control) versus CBD treatment. (f) Western blot for p-ERK1/2, total ERK1/2, and β tubulin (loading control) in ASZ_ERRasV12 and UWBC_ERRasV12 upon doxycycline/4OHT after transfection with ns_siRNA versus OFD1_siRNA. Scale bar = 25 µm. Horizontal and error bars in e represent the mean ± standard deviation. **P* < 0.05, ***P* < 0.01, ****P* < 0.001. 4OHT, 4-hydroxy-tamoxifen; CBD, ciliobrevin D; ctrl, control; Dox, doxycycline; GSEA, Gene Set Enrichment Analysis; HH, Hedgehog; M, mol/L; NES, normalized enrichment score; ns, non-silencing; p-, phosphorylated; RNAseq, RNA sequencing; siRNA, small interfering RNA.

activation by itself. We thus hypothesized that loss of cilia sustains pathway activity once activated. Therefore, we subcloned the previously reported 4-hydroxy-tamoxifen (4OHT)–dependent constitutive RasV12 (Dajee et al., 2002) under the doxycycline (Dox)-inducible promoter in the piggyBac transposon vector. Stable transfections were performed

in both the Smoⁱ-sensitive 3T3 cell line and Smoⁱ-resistant ASZ and UWBC BCC cell lines. As shown by Western blot for p-ERK1/2 and p-MEK immunostaining (as readout for Ras/MAPK pathway activation), all three obtained cell lines showed inducible Ras pathway activation upon Dox and 4OHT stimulation (see Supplementary Figure S4a–d). Levels

of Ras/MAPK induction were similar to those in human SCC cell line SCC-13 (see [Supplementary Figure S4e](#) and [f](#)), confirming physiological activation of the Ras/MAPK pathway. To test the effect of the loss of cilia on the activated Ras/MAPK pathway, we performed RNA sequencing on ASZ_ERRasV12/Dox-4OHT upon either DMSO (control) or CBD (10 $\mu\text{mol/L}$) (GEO accession number GSE120954). In this setting, GSEA showed a significant positive enrichment for Ras signaling in CBD-treated cells ([Figure 3b](#)), suggesting that loss of cilia potentiates Ras pathway activation. This result was confirmed by Western blot for p-ERK1/2. Whereas CBD treatment did not affect ERK1/2 phosphorylation on ASZ_ERRasV12 or UWBC_ERRasV12, it did enhance ERK1/2 phosphorylation upon concomitant Ras pathway activation through Dox/4OHT stimulation ([Figure 3c](#), and see [Supplementary Figure S5a](#) online). Similar observations were made using p-MEK immunostaining ([Figure 3d](#) and [e](#)). The higher individual values (at the cellular level) of MEK phosphorylation observed in both ASZ_ERRasV12/Dox-4OHT and UWBC_ERRasV12/Dox upon CBD treatment compared with control (DMSO) suggest a potentiation of Ras pathway activation rather than a selection process. As an alternative approach to pharmacological depletion of primary cilia, we measured p-ERK1/2 level by Western blot in ASZ_ERRasV12 and UWBC_ERRasV12 previously treated with either non-silencing or OFD1 small interfering RNAs. OFD1 small interfering RNA efficiently potentiated Ras/MAPK pathway activation induced upon Dox-4OHT stimulation in both ASZ and UWBC cell lines ([Figure 3f](#), and see [Supplementary Figure S5b](#)), confirming the role of primary cilia in antagonizing Ras/MAPK pathway activity.

HH-to-Ras/MAPK pathway switching confers resistance to canonical and noncanonical HH pathway inhibitors and sensitivity to MEK inhibitor UO126 in vitro

Finally, we interrogated the extent to which pathway switching affects BCC sensitivity to targeted therapy. We first tested the effect of Ras pathway activation on sensitivity to Smoⁱ, using the 3T3_ERRasV12, which shows physiological sensitivity to vismodegib upon stimulation with Smoothed agonist. Smoothed agonist -induced sensitivity to vismodegib was lost upon concomitant activation of the Ras pathway ([Figure 4a](#)). To determine whether this effect was Smoⁱ specific, we then induced Ras pathway activation under HH pathway inhibitors acting downstream of Smo inhibition, in both ASZ and UWBC BCC cell lines. Similarly, Ras pathway activation in ASZ_ERRasV12 and UWBC_ERRasV12 conferred resistance to both PSI (an aPKC inhibitor, acting downstream of Smo ([Mirza et al., 2017](#))) and CCG1423 (an MRTF inhibitor, implicated in noncanonical HH pathway activation ([Whitson et al., 2018](#))), as illustrated by the right shift of the half-maximal inhibitory concentration values ([Figure 4b](#) and [c](#)). Although noncanonical HH inhibitors have not been tested in clinical practice yet, these results suggest that HH-to-Ras pathway switching may confer a cell state distinct from that driven by canonical or noncanonical HH activation. To test this idea, we investigated whether resistance to HH inhibitors might be overcome by Ras/MAPK inhibition. Indeed, both ASZ_ERRasV12 and UWBC_ERRasV12 cell lines were sensitive to MEK inhibitor UO126 upon Ras pathway activation,

as illustrated by the left shift of the half-maximal inhibitory concentration values ([Figure 4d](#)).

Altogether, these results identify HH-to-Ras/MAPK pathway switching as a mechanism for BCC resistance distinct from both canonical and noncanonical HH pathway activation and MAPK inhibition as a promising therapy to prevent BCC escape from HH inhibition. They identify the primary cilia as key regulators of this switch.

DISCUSSION

Here, we show the correlation of resistance with loss of the primary cilium and the antagonistic relationship between the primary cilium and Ras/MAPK activity, thereby providing insight into BCC pathway switching and resistance to Smoⁱ.

Our work provides an important contrast to previous mechanisms because we found an accumulation of mutations in genes encoding components of the primary cilia, reduced numbers of cells with primary cilium, reduced HH pathway output, and activation of Ras/MAPK signaling. The cilium is composed of over 300 proteins that must work together for proper HH signaling ([van Dam et al., 2013](#)). The frequency of recurrent coding region variants that include nonsense and small deletions argues for the existence of mutations of more than one ciliary protein in each tumor cell and a reduction in ciliary function. However, because of the observed complex ciliary genotypes, we can only speculate as to the precise phenotype in each cell, especially given the known functional variability of each genotype in distinct biological contexts ([Arnaiz et al., 2014](#)). This complexity likely explains the observed sporadic loss of full-length mature cilia despite the frequency of ciliary mutations.

Elevated mutation frequencies of ciliome genes have been detected in other advanced cancers, including breast carcinoma ([Menzl et al., 2014](#)), melanoma ([Zingg et al., 2018](#)), ovarian cancer ([Egeberg et al., 2012](#)), and thyroid cancer ([Lee et al., 2018](#); [Menzl et al., 2014](#)), suggesting that the cilia may function to enforce particular lineages or cell states outside the skin. Recently, [Zhao et al. \(2017\)](#) identified mutations in ciliary genes conferring resistance to sonidegib in medulloblastoma ([Zhao et al., 2017](#)). In their model, HH pathway reduction upon loss of cilia induces tumor cells to go into a persist state, where low proliferation rate reduces sensitivity to Smoⁱ and allows for further HH pathway-activating genetic alterations to accumulate. Here, we show that loss of cilia, in addition to reducing HH pathway activation, appears permissive for the dominant oncogenic Ras/MAPK pathway, which is involved in both skin differentiation ([Dajee et al., 2002](#); [Dlugosz et al., 1994](#); [Lin and Lowe, 2001](#); [Mainiero et al., 1997](#)) and SCC carcinogenesis ([Dajee et al., 2003](#); [To et al., 2005](#); [Woodworth et al., 2004](#)). Our data indicate that Ras pathway activation constitutes a distinct state, because it confers resistance to both canonical and noncanonical HH inhibitors. We may thus reasonably expect Ras activation to appear upon and confer resistance to the newly approved HH inhibitor sonidegib ([Danial et al., 2016](#); [Migden et al., 2015](#)) or the preclinical HH inhibitors currently in development. Here, as a proof-of-principle for the use of MAPK inhibitors for the treatment of BCC, we show that Ras activation in BCC cell lines actually confers sensitivity to p-MEK inhibitor UO126. However, given the

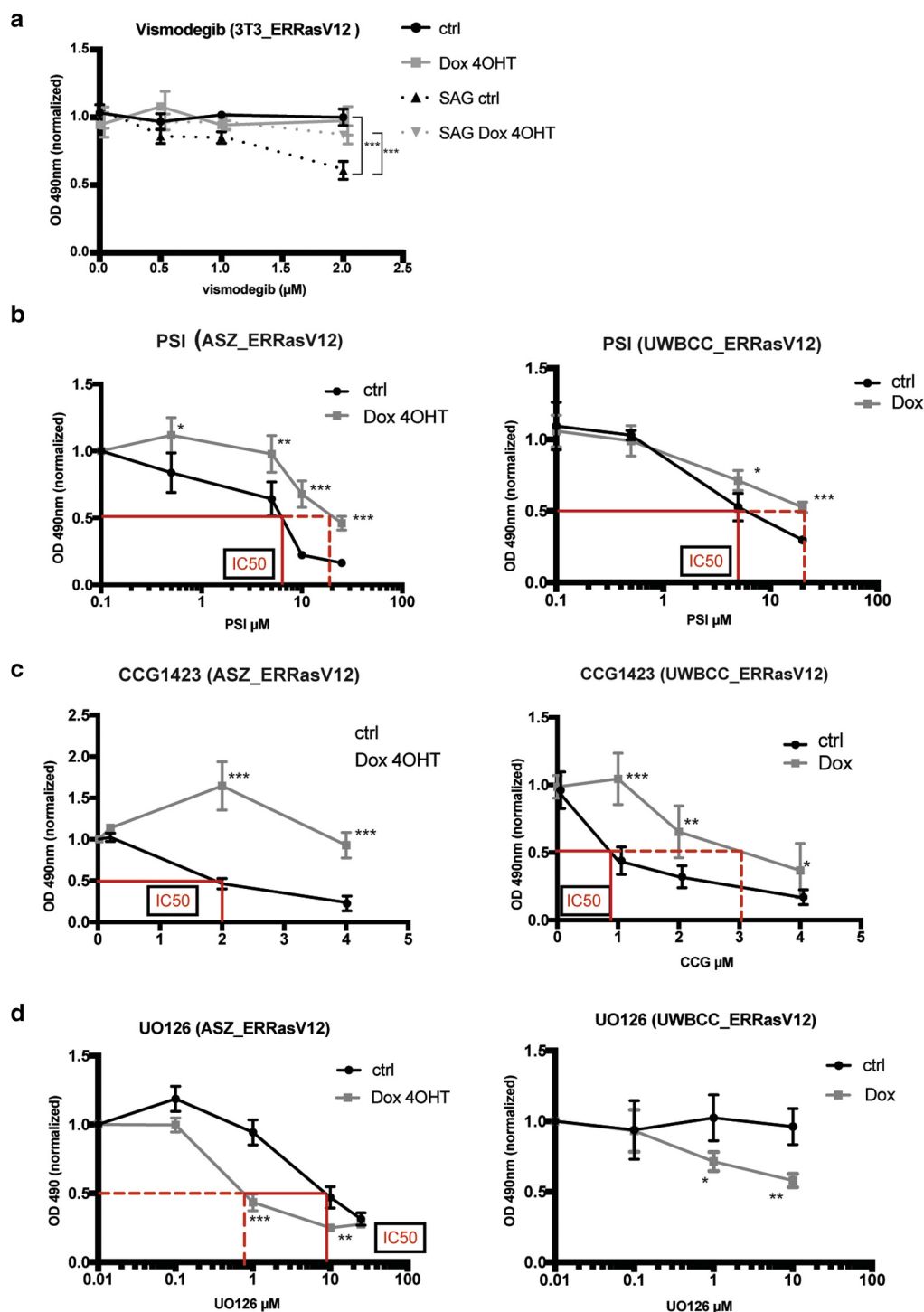


Figure 4. HH-to-Ras pathway switching confers resistance to canonical and noncanonical HH pathway inhibitors and sensitivity to MEK inhibitor UO126 in vitro. (a) Vismodegib sensitivity assessed by MTT assay in 3T3_ERRasV12 upon stimulation with Smoothed agonist (100 nmol/L) and doxycycline/4OHT. (b) PSI (aPKC inhibitor) sensitivity assessed by MTT assay in ASZ_ERRasV12 and UWBC_ERRasV12 upon doxycycline/4OHT. (c) CCG1423 (MRTF inhibitor) sensitivity assessed by MTT assay in ASZ_ERRasV12 or UWBC_ERRasV12 upon doxycycline/4OHT. (d) UO126 (MEK inhibitor) sensitivity assessed by MTT assay in ASZ_ERRasV12 or UWBC_ERRasV12 upon doxycycline/4OHT. When reached, half-maximal inhibitory concentration are indicated in red lines, both in the absence (full line) or presence (dashed line) of doxycycline/4OHT. Dots and error bars represent the mean \pm standard deviation for $n \geq 6$ per group. * $P < 0.05$, ** $P < 0.01$ *** $P < 0.001$. 4OHT, 4-hydroxy-tamoxifen; aPKC, atypical protein kinase C; ctrl, control; Dox, doxycycline; HH, Hedgehog; IC50, half-maximal inhibitory concentration; M, mol/L; MEK, MAPK/ERK kinase; MTT, 3-(4,5-dimethylthiazol-2-yl)-2,5-diphenyltetrazolium bromide; OD, optical density; SAG, Smoothed agonist.

existence of rapid resistance or limited efficiency of Smo and Ras/MAPK inhibitors in clinical trials of patients with non-syndromic tumors (Axelson et al., 2013; Santarpia et al., 2012; Sekulic et al., 2012), an alternative strategy may consist in targeting the crosstalk between cilia and the Ras/MAPK pathway, thereby potentially preventing pathway switching and reducing the frequency of resistance. Our data did not identify the mechanism of Ras/MAPK regulation by primary cilia. Abdul-Majeed and Nauli (2011) reported that, in polycystic kidney disease, reduced intracellular Ca^{2+}

resulting from reduced ciliogenesis decreases phosphodiesterase 1-mediated conversion of cAMP to adenosine monophosphate, inducing downstream MAPK target activation (Abdul-Majeed and Nauli, 2011). Alternatively, Ras pathway activation was reported to induce primary cilia disassembly and reduce HH pathway activation through the induction of Aurora kinase and Dyrk1b, respectively (Furukawa et al., 2006; Kobayashi et al., 2017; Lauth et al., 2010; Seeley et al., 2009), suggesting that restoring ciliogenesis may restore sensitivity to HH inhibition. These mechanisms,

however, need to be further validated experimentally in BCC. Therefore, experimental models fully recapitulating the BCC-to-SCC transition will be required to help decipher the implication of primary cilia both dynamically and mechanistically in this intriguing process.

In conclusion, this work identifies the pathway switching from HH to Ras/MAPK as a further mechanism of resistance in BCCs treated with Smoⁱ, emphasizing the need for combined and tailored targeted therapies as BCCs display various ways to escape Smo inhibition. We bring experimental evidence for the role of primary cilia as pivotal regulators of the antagonistic HH and Ras/MAPK pathways, thereby opening perspectives for the treatment of advanced resistant BCC.

MATERIAL AND METHODS

Human samples

The study on human paraffin samples was performed with approval from the Stanford University institutional review board, protocol 18325 (Stanford, CA), with a waiver of written, informed consent from participants for the paraffin blocks. Histological diagnoses of Gorlin syndrome patients and sporadic naive and resistant BCC samples used in this study were previously confirmed in Chiang et al., (2018) and Atwood et al. (2015). Histological diagnoses of BCC and SCC samples used for Gli1 and p-MEK immunostainings were confirmed by an independent dermatopathologist.

Whole-exome sequencing and analysis

Gene ontology analysis was performed with Panther 13.1 (University of South California, Los Angeles, CA) using the Gene Ontology annotations database (released February 2, 2018) on the list of previously identified genes specifically mutated in resistant BCC compared with normal skin (GEO accession number GSE58377) (Atwood et al., 2015). Ciliome mutations were quantified from whole-exome sequencing data from 21 Gorlin syndrome patients, 12 sporadic BCCs, and 12 resistant BCCs, and normal skin pairs were previously obtained as described by Chiang et al. (2018) and Atwood et al. (2015) and deposited under National Institutes of Health Sequence Read Archive SAMN07507265–SAMN07507288 and GEO GSE58377 accession numbers, respectively. Custom scripts were written to count the total number of mutations in a specified set of cilia gene known to be important in cilia function (ciliome) (van Dam et al., 2013) and to calculate the lengths of these genes. Ciliome mutations were quantified as the number of mutations per Mb of the whole ciliome (1.303754/Mb).

Cell lines and cell culture

ASZ001 cells (mouse BCC cell line) were grown in M154CF (Thermo Fisher Scientific, Waltham, MA) supplemented with 2% chelated fetal bovine serum, 1% penicillin/streptomycin and 0.05 mmol/L CaCl₂ (So et al., 2006). UWBC cells (human BCC cell line) were grown in EpilifeCF (Thermo Fisher Scientific) supplemented with 7% chelated fetal bovine serum, 1% penicillin/streptomycin, and 0.05 mmol/L CaCl₂ (Noubissi et al., 2014). NIH-3T3 were grown in DMEM (Thermo Fisher Scientific) supplemented with 10% fetal bovine serum and 1% penicillin/streptomycin. SCC-13 SCC cells (human SCC cell line) were generously provided by C. Lee (Stanford, CA) and grown in KSFM (Thermo Fisher Scientific) supplemented with 1% penicillin/streptomycin, 0.25 µg/ml bovine pituitary extract, 0.2 ng/ml epidermal growth factor, and 0.3 mmol/L CaCl₂ (Thermo Fisher Scientific). Experiments were carried out in serum-starved conditions.

RNA sequencing and analysis

RNA samples were obtained from adherent cells with the RNeasy kit from Qiagen (Germantown, MD) according to manufacturer's instructions. Library preparation, sequencing, and mapping were performed as described previously (Atwood et al., 2015). Alignment was performed using TopHat (John Hopkins University, Baltimore, MD) with mm9 as a reference genome. The DESeq R package (R Core Team, Vienna, Austria) was used to generate a preranked list of genes differentially expressed in ASZ with or without CBD or ASZERRasV12/Dox-4OHT with or without CBD before submission to GSEA2.2.4 software (Broad Institute, Cambridge, MA) for HH or Ras pathway enrichment. Mouse RNA sequencing data generated in this study were submitted to GEO (GSE120954). An additional GSEA was carried out using RNA-sequencing data from published human resistant and sensitive BCCs (GEO accession number 58377 [Atwood et al., 2015]). For gene expression, resistant BCCs were compared with sensitive BCCs obtained from the same patient. Genes differentially expressed were preranked according to log₂ fold change before submission to GSEA2.2.4 software for HH or Ras pathway enrichment.

MTT assays

For MTT (3-[4,5-dimethylthiazol-2-yl]-2,5-diphenyltetrazolium bromide) assays, Ras pathway activation was obtained by using medium containing Dox and 4-OHT. After 24 hours, the medium was replaced with medium containing DMSO or the tested compound and incubated for 48 hours. Cell viability was measured using CellTiter 96 Aqueous One Solution (Promega, Madison, WI) and normalized to control (DMSO-treated cells). Each condition was tested six times. For each drug and cell line, the half-maximal inhibitory concentration was determined as the drug concentration giving the half-maximal response compared with the control (DMSO-treated) conditions. CBD (Sigma-Aldrich, St. Louis, MO), vismodegib (GDC-0449; Selleckchem, Houston, TX), CCG1423 (Cayman Chemicals, Ann Harbor, MI), and PSI (2549; Tocris, Minneapolis, MN) were suspended in DMSO.

Statistical analyses

Statistical comparisons were performed by a two-tailed Student *t* test or one-way analysis of variance with Tukey posttest for multiple comparisons. Statistical analyses were performed using GraphPad Prism (GraphPad, San Diego, CA). The data were considered to be significantly different when *P* was less than 0.05.

A more complete and detailed description of the methods is included in [Supplementary Materials and Methods](#).

CONFLICT OF INTEREST

The authors state no conflict of interest.

ACKNOWLEDGMENTS

This work was supported by an Swiss National Science Foundation fellowship (to FK), a Fondation René Touraine fellowship (to FK), F32 CA200108-01 National Institutes of Health grant (to NH), and National Institutes of Health R01 ARO46786 and ARO54780 (to AEO).

AUTHOR CONTRIBUTIONS

FK and NH performed in vitro and ex vivo experiments. FK, NH, GS, PJ, SA, and KYS performed in silico analyses. RJW performed in vitro experiments. KR provided histological diagnoses. FK and AEO prepared the figures and drafted the manuscript.

SUPPLEMENTARY MATERIAL

Supplementary material is linked to the online version of the paper at www.jidonline.org, and at <https://doi.org/10.1016/j.jid.2018.11.035>.

REFERENCES

- Abdul-Majeed S, Nauli SM. Calcium-mediated mechanisms of cystic expansion. *Biochim Biophys Acta* 2011;1812:1281–90.
- Arnaiz O, Cohen J, Tassin AM, Koll F. Remodeling Cildb, a popular database for cilia and links for ciliopathies. *Cilia* 2014;3:9.
- Atwood SX, Li M, Lee A, Tang JY, Oro AE. GLI activation by atypical protein kinase C ι/λ regulates the growth of basal cell carcinomas. *Nature* 2013;494(7438):484–8.
- Atwood SX, Sarin KY, Whitson RJ, Li JR, Kim G, Rezaee M, et al. Smoothed variants explain the majority of drug resistance in basal cell carcinoma. *Cancer Cell* 2015;27:342–53.
- Axelsson M, Liu K, Jiang X, He K, Wang J, Zhao H, et al. U.S. Food and Drug Administration approval: vismodegib for recurrent, locally advanced, or metastatic basal cell carcinoma. *Clin Cancer Res* 2013;19:2289–93.
- Bangs F, Anderson KV. Primary cilia and mammalian Hedgehog signaling. *Cold Spring Harb Perspect Biol* 2017;9(5):a028175.
- Bonilla X, Parmentier L, King B, Bezrukov F, Kaya G, Zoete V, et al. Genomic analysis identifies new drivers and progression pathways in skin basal cell carcinoma. *Nat Genet* 2016;48:398–406.
- Buonamici S, Williams J, Morrissey M, Wang A, Guo R, Vattay A, et al. Interfering with resistance to smoothed antagonists by inhibition of the PI3K pathway in medulloblastoma. *Sci Transl Med* 2010;2(51):51ra70.
- Chandarlapaty S. Negative feedback and adaptive resistance to the targeted therapy of cancer. *Cancer Discov* 2012;2:311–9.
- Chandarlapaty S, Sawai A, Scaltriti M, Rodrik-Outmezguine V, Grbovic-Huezo O, Serra V, et al. AKT inhibition relieves feedback suppression of receptor tyrosine kinase expression and activity. *Cancer Cell* 2011;19:58–71.
- Chang AL, Oro AE. Initial assessment of tumor regrowth after vismodegib in advanced basal cell carcinoma. *Arch Dermatol* 2012;148:1324–5.
- Chiang A, Jaju PD, Batra P, Rezaee M, Epstein EH Jr, Tang JY, et al. Genomic stability in syndromic basal cell carcinoma. *J Invest Dermatol* 2018;138:1044–51.
- Dajee M, Lazarov M, Zhang JY, Cai T, Green CL, Russell AJ, et al. NF- κ B blockade and oncogenic Ras trigger invasive human epidermal neoplasia. *Nature* 2003;421(6923):639–43.
- Dajee M, Tarutani M, Deng H, Cai T, Khavari PA. Epidermal Ras blockade demonstrates spatially localized Ras promotion of proliferation and inhibition of differentiation. *Oncogene* 2002;21:1527–38.
- Daniel C, Sarin KY, Oro AE, Chang AL. An investigator-initiated open-label trial of sonidegib in advanced basal cell carcinoma patients resistant to vismodegib. *Clin Cancer Res* 2016;22:1325–9.
- Dijkgraaf GJ, Aliche B, Weinmann L, Januario T, West K, Modrusan Z, et al. Small molecule inhibition of GDC-0449 refractory smoothed mutants and downstream mechanisms of drug resistance. *Cancer Res* 2011;71:435–44.
- Dlugosz AA, Cheng C, Williams EK, Dharia AG, Denning MF, Yuspa SH. Alterations in murine keratinocyte differentiation induced by activated *ras^{Ha}* genes are mediated by protein kinase C- α . *Cancer Res* 1994;54:6413–20.
- Egeberg DL, Lethan M, Manguso R, Schneider L, Awan A, Jørgensen TS, et al. Primary cilia and aberrant cell signaling in epithelial ovarian cancer. *Cilia* 2012;1:15.
- Epstein EH. Basal cell carcinomas: attack of the hedgehog. *Nat Rev Cancer* 2008;8:743–54.
- Ferrante MI, Zullo A, Barra A, Bimonte S, Messaddeq N, Studer M, et al. Oral-facial-digital type I protein is required for primary cilia formation and left-right axis specification. *Nat Genet* 2006;38:112–7.
- Fu W, Asp P, Canter B, Dynlacht BD. Primary cilia control hedgehog signaling during muscle differentiation and are deregulated in rhabdomyosarcoma. *Proc Natl Acad Sci USA* 2014;111:9151–6.
- Furukawa T, Kanai N, Shiwaku HO, Soga N, Uehara A, Horii A. AURKA is one of the downstream targets of MAPK1/ERK2 in pancreatic cancer. *Oncogene* 2006;25:4831–9.
- Gerdes MJ, Myakishev M, Frost NA, Rishi V, Moitra J, Acharya A, et al. Activator protein-1 activity regulates epithelial tumor cell identity. *Cancer Res* 2006;66:7578–88.
- Kasper M, Jaks V, Hohl D, Toftgard R. Basal cell carcinoma—molecular biology and potential new therapies. *J Clin Invest* 2012;122:455–63.
- Kobayashi T, Nakazono K, Tokuda M, Mashima Y, Dynlacht BD, Itoh H. HDAC2 promotes loss of primary cilia in pancreatic ductal adenocarcinoma. *EMBO Rep* 2017;18:334–43.
- Lauth M, Bergström Å, Shimokawa T, Tostar U, Jin Q, Fendrich V, et al. DYRK1B-dependent autocrine-to-paracrine shift of Hedgehog signaling by mutant RAS. *Nat Struct Mol Biol* 2010;17:718–25.
- Lee CS, Bhaduri A, Mah A, Johnson WL, Ungewickell A, Aros CJ, et al. Recurrent point mutations in the kinetochore gene *KNSTRN* in cutaneous squamous cell carcinoma. *Nat Genet* 2014;46:1060–2.
- Lee J, Yi S, Won M, Song YS, Yi HS, Park YJ, et al. Loss-of-function of IFT88 determines metabolic phenotypes in thyroid cancer. *Oncogene* 2018;37:4455–74.
- Lefort K, Mandinova A, Ostano P, Kolev V, Calpini V, Kolfschoten I, et al. Notch1 is a p53 target gene involved in human keratinocyte tumor suppression through negative regulation of ROCK1/2 and MRCK α kinases. *Genes Dev* 2007;21:562–77.
- Lin AW, Lowe SW. Oncogenic *ras* activates the ARF-p53 pathway to suppress epithelial cell transformation. *Proc Natl Acad Sci USA* 2001;98:5025–30.
- Mainiero F, Murgia C, Wary KK, Curatola AM, Pepe A, Blumemberg M, et al. The coupling of α 6 β 4 integrin to Ras-MAP kinase pathways mediated by Shc controls keratinocyte proliferation. *EMBO J* 1997;16:2365–75.
- Menzl I, Lebeau L, Pandey R, Hassounah NB, Li FW, Nagle R, et al. Loss of primary cilia occurs early in breast cancer development. *Cilia* 2014;3:7.
- Migden MR, Guminski A, Gutzmer R, Dirix L, Lewis KD, Combemale P, et al. Treatment with two different doses of sonidegib in patients with locally advanced or metastatic basal cell carcinoma (BOLT): a multi-centre, randomised, double-blind phase 2 trial. *Lancet Oncol* 2015;16:716–28.
- Mirza AN, Fry MA, Urman NM, Atwood SX, Roffey J, Ott GR, et al. Combined inhibition of atypical PKC and histone deacetylase 1 is cooperative in basal cell carcinoma treatment. *JCI Insight* 2017;2(21):e97071.
- Noubissi FK, Kim T, Kawahara TN, Aughenbaugh WD, Berg E, Longley BJ, et al. Role of CRD-BP in the growth of human basal cell carcinoma cells. *J Invest Dermatol* 2014;134:1718–24.
- Otsuka A, Dreier J, Cheng PF, Nageli M, Lehmann H, Felderer L, et al. Hedgehog pathway inhibitors promote adaptive immune responses in basal cell carcinoma. *Clin Cancer Res* 2015;21:1289–97.
- Pak E, Segal RA. Hedgehog signal transduction: key players, oncogenic drivers, and cancer therapy. *Dev Cell* 2016;38:333–44.
- Pickering CR, Zhou JH, Lee JJ, Drummond JA, Peng SA, Saade RE, et al. Mutational landscape of aggressive cutaneous squamous cell carcinoma. *Clin Cancer Res* 2014;20:6582–92.
- Ransohoff KJ, Tang JY, Sarin KY. Squamous change in basal-cell carcinoma with drug resistance. *N Engl J Med* 2015;373:1079–82.
- Rubin LL, de Sauvage FJ. Targeting the Hedgehog pathway in cancer. *Nat Rev Drug Discov* 2006;5:1026–33.
- Saintes C, Saint-Jean M, Brocard A, Peuvrel L, Renaut JJ, Khammari A, et al. Development of squamous cell carcinoma into basal cell carcinoma under treatment with vismodegib. *J Eur Acad Dermatol Venereol* 2015;29:1006–9.
- Santarpia L, Lippman SM, El-Naggar AK. Targeting the MAPK-RAS-RAF signaling pathway in cancer therapy. *Expert Opin Ther Targets* 2012;16:103–19.
- Seeley ES, Carriere C, Goetze T, Longnecker DS, Korc M. Pancreatic cancer and precursor pancreatic intraepithelial neoplasia lesions are devoid of primary cilia. *Cancer Res* 2009;69:422–30.
- Sekulic A, Migden MR, Oro AE, Dirix L, Lewis KD, Hainsworth JD, et al. Efficacy and safety of vismodegib in advanced basal-cell carcinoma. *N Engl J Med* 2012;366:2171–9.
- Serra V, Scaltriti M, Prudkin L, Eichhorn PJ, Ibrahim YH, Chandarlapaty S, et al. PI3K inhibition results in enhanced HER signaling and acquired ERK dependency in HER2-overexpressing breast cancer. *Oncogene* 2011;30:2547–57.
- Sharpe HJ, Pau G, Dijkgraaf GJ, Basset-Seguín N, Modrusan Z, Januario T, et al. Genomic analysis of smoothed inhibitor resistance in basal cell carcinoma. *Cancer Cell* 2015;27:327–41.
- So PL, Langston AW, Daniellinia N, Hebert JL, Fujimoto MA, Khaimskiy Y, et al. Long-term establishment, characterization and manipulation of cell lines from mouse basal cell carcinoma tumors. *Exp Dermatol* 2006;15:742–50.

F Kuonen et al.

Pathway Switching as a Mechanism of Resistance in Basal Cell Carcinoma

- Tang JY, Mackay-Wiggan JM, Aszterbaum M, Yauch RL, Lindgren J, Chang K, et al. Inhibiting the hedgehog pathway in patients with the basal-cell nevus syndrome. *N Engl J Med* 2012;366:2180–8.
- To MD, Perez-Losada J, Mao JH, Balmain A. Crosstalk between Pten and Ras signaling pathways in tumor development. *Cell Cycle* 2005;4:1185–8.
- van Dam TJ, Wheway G, Slaats GG, Group SS, Huynen MA, Giles RH. The SYSCILIA gold standard (SCGSv1) of known ciliary components and its applications within a systems biology consortium. *Cilia* 2013;2:7.
- Whitson RJ, Lee A, Urman NM, Mirza A, Yao CY, Brown AS, et al. Noncanonical hedgehog pathway activation through SRF-MKL1 promotes drug resistance in basal cell carcinomas. *Nat Med* 2018;24:271–81.
- Woodworth CD, Michael E, Smith L, Vijayachandra K, Glick A, Hennings H, et al. Strain-dependent differences in malignant conversion of mouse skin tumors is an inherent property of the epidermal keratinocyte. *Carcinogenesis* 2004;25:1771–8.
- Wu F, Zhang Y, Sun B, McMahon AP, Wang Y. Hedgehog signaling: from basic biology to cancer therapy. *Cell Chem Biol* 2017;24:252–80.
- Yauch RL, Dijkgraaf GJ, Alicke B, Januario T, Ahn CP, Holcomb T, et al. Smoothed mutation confers resistance to a Hedgehog pathway inhibitor in medulloblastoma. *Science* 2009;326(5952):572–4.
- Zhao X, Pak E, Ornell KJ, Pazyra-Murphy MF, MacKenzie EL, Chadwick EJ, et al. A transposon screen identifies loss of primary cilia as a mechanism of resistance to SMO inhibitors. *Cancer Discov* 2017;7:1436–49.
- Zhao X, Ponomaryov T, Ornell KJ, Zhou P, Dabral SK, Pak E, et al. RAS/MAPK activation drives resistance to Smo inhibition, metastasis, and tumor evolution in Shh pathway-dependent tumors. *Cancer Res* 2015;75:3623–35.
- Zingg D, Debbache J, Pena-Hernandez R, Antunes AT, Schaefer SM, Cheng PF, et al. EZH2-mediated primary cilium deconstruction drives metastatic melanoma formation. *Cancer Cell* 2018;34:69–84.